PHYSICAL REVIEW B VOLUME 35, NUMBER 13 1 MAY 1987

Raman scattering in antiferromagnetic $FePS_3$ and $FePSe_3$ crystals

M. Scagliotti,* M. Jouanne, and M. Balkanski
Laboratoire de Physique des Solides, Université Pierre et Marie Curie, 4 place Jussieu, 75252 Paris Cedex 05, France

G. Ouvrard
Laboratoire de Chimie des Solides, 2 rue de La Houssinière, 44072 Nantes Cedex, France

G. Benedek
Dipartimento di Fisica dell'Università and Gruppo Nazionale di Struttura della Materia del Consiglio Nazionale delle Ricerche, via Celoria 16, 20133 Milano, Italy
(Received 2 September 1986)

Raman spectra of iron phosphorus trichalcogenide crystals ($FePX_3$, X = S,Se) are measured, and a compilation of the peak frequencies is given. The spectral features due to first-order phonon Raman scattering are analyzed and assigned. At low temperatures in iron phosphorus trisulfide the vibrational Raman-scattering efficiency displays an anomalous enhancement and new structures appear. The temperature dependence of the integrated intensity, bandwidth, and frequency of the Raman peaks is studied and correlated with the antiferromagnetic ordering. It is found that the spin superstructure produces a folding of the phonon dispersion curves into the center of the Brillouin zone and activates new phonon modes in the Raman spectrum.

INTRODUCTION

Iron phosphorus trisulfide is a good example of a two-dimensional (2D) Ising-type antiferromagnet with the magnetic ions arranged in a honeycomb lattice. It exhibits, around 118 K, a magnetic phase transition from the paramagnetic phase to an ordered phase in which ferromagnetic linear chains are coupled to each other antiferromagnetically in the *ab* plane.[1,2] Similar magnetic properties are found in iron phosphorus triselenide.[3] At present these layered compounds, as well as nickel phosphorus trisulfide, are the object of intense studies for their interesting magnetic properties[1-5] and for their promising performances as lithium-battery electrodes.[6-8]

Recently, spin-dependent phonon Raman scattering in $FePS_3$ has been reported.[9] In the present work, the effects of the magnetic ordering on the Raman spectra of iron phosphorus trichalcogenides are extensively investigated, and new details on the lattice dynamics are obtained by studying the low-temperature spectra.

Despite the low scattered intensity and the opacity of these compounds, Raman spectra are measured with good spectral resolution on cleaved single crystals, and cross and parallel polarization of the scattered light are analyzed. A complete compilation of the Raman frequencies is given, and the previous peak assignments[9,10] are reconsidered and corrected. The Raman spectra of iron phosphorus triselenide are reported for what we believe is the first time, and the effects of the selenium-sulfur substitution are briefly discussed. Dramatic changes in the phonon peak intensities are observed at low temperatures only in the Raman spectrum of iron phosphorus trisulfide. The peak intensities, bandwidths, and frequencies are measured at various temperatures between 4.2 and 300 K, and a correlation between the Raman tensor and the antiferromagnetic order is found.

Anomalous intensity enhancements and the abrupt appearance of zone-center phonon peaks which are forbidden in the paramagnetic phase can be observed in the Raman spectra of magnetic crystals at the onset of the magnetic ordering.[11] Also zone boundary phonons can be activated by the magnetic ordering if the magnetic superstructure can assure the momentum conservation.[12-14] The intensity of the enhanced peaks depends on the temperature like the spin-correlation function of the crystal.[11] The spin-dependent and the spin-independent Raman scattering have generally different selection rules and resonant behaviors,[11] so that the study of the low temperature phonon Raman spectrum in magnetic crystals can provide new details on the lattice dynamics.

Until now, however, the spin-dependent phonon Raman scattering has not received adequate attention. Only some experimental works[12-19] and a few theoretical studies[11] have been published on the subject. This fact has stimulated the present investigation of the Raman scattering in transition-metal phosphorus trichalcogenides around the magnetic transition.

EXPERIMENTAL

The Raman measurements are carried out on iron phosphorus trichalcogenide single crystals. The samples are cleaved to obtain a surface with good optical quality, and immediately placed under vacuum in a temperature variable SMC-TBT cryostat. The temperature is measured by means of a silicon diode on the copper sample holder.

The Raman spectra are excited by Kr^+ and Ar^+ laser lines in a quasibackscattering geometry with the laser beam at Brewster-angle incidence. To avoid sample heating by the laser beam only few tens of milliwatts are used in these experiments. The scattered light is dispersed by means of a double-grating Coderg PH1 spectrometer and

the signal is analyzed by a conventional photon-counting system. The spectral resolution is about 1.1 cm^{-1} in the bandwidth measurements and of about 6.7 cm^{-1} in the integrated intensity measurements.

The samples used in the present work are characterized by differential scanning calorimetry (DSC) in the temperature range 90–300 K. These measurements are made by means of a Perkin Elmer DSC-II calorimeter. A λ-type peak is observed in the DCS traces of $FePS_3$ and $FePSe_3$ at 118 and 106 K, respectively.[20]

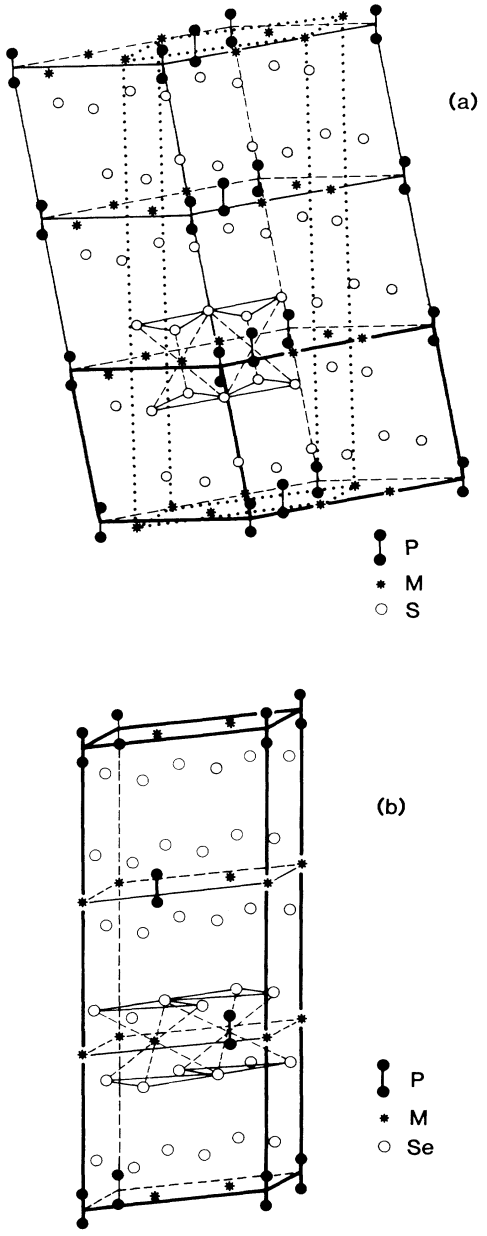

FIG. 1. Unit cell of the iron phosphorus trisulfide (a) and of the iron phosphorus triselenide (b).

CRYSTALLOGRAPHIC AND MAGNETIC STRUCTURE

Iron phosphorus trisulfide is a layered compound with the $AlCl_3$ structure[21] where the empty intralayer anion octahedra are filled by phosphorus dimers. As shown in Fig. 1(a) this structure originates from a small monoclinic distortion of the rhombohedral $CrCl_3$ structure. Hexagonal sulfur sheets are arranged along the c axis in an ABC stacking and each transition-metal cation has three cationic neighbors in the same sheet and two in each adjacent sheet. The monoclinic unit cell contains a single layer and four formula units. The lattice parameters are $a=5.934$ Å, $b=10.28$ Å, $c=6.772$ Å, and $\beta=107.2°$.[22,23] The structure parameters of $FePS_3$ and of other MPS_3 compounds have been recently determined and correlated with their chemical properties by Brec and co-workers.[24]

$FePSe_3$ is somewhat different from $FePS_3$. It belongs to the rhombohedral $FeCl_3$ structure, with the phosphorus dimers filling the empty intralayer octahedra and no monoclinic distortion. The selenium layers are stacked along the c axis in an AB sequence; iron ions display the same arrangement in the sheet, but have only one iron neighbor on an adjacent layer [Fig. 1(b)]. The rhombohedral unit cell contains three layers and six molecules. The lattice parameters are $a=6.265$ Å, $c=19.80$ Å, and $\gamma=120°$.[22,23]

The magnetic cell of the trisulfide is doubled along the c axis with respect to the crystallographic one, but it is unchanged in the ab plane.[2] In the triselenide the magnetic cell is doubled both along the a and c directions as compared to the crystallographic one, and the symmetry is then lowered from rhombohedral to triclinic.[3]

RAMAN SPECTRA

Despite the complex unit cell the Raman spectra can be interpreted by considering a simple pseudocell containing one P_2X_6 anion and two iron cations.[10] The P_2X_6 anion normal modes and the metal cation vibrations will be observed. The staggered P_2X_6 molecule belongs to the D_{3d} symmetry group and six Raman active modes are expected: three A_{1g}-type modes (polarized) and three E_g-type modes (depolarized) (see Fig. 2).[25]

This simple picture is supported by the following effects.

(a) The spectral pattern in the 150–600 cm^{-1} frequency region is not affected by the metal cation substitution and is very similar to that of $Na_4P_2S_6$ aqueous solutions, which contains free $(P_2S_6)^{4-}$ anions.[10]

(b) The pattern systematically shifts to lower frequencies when selenium substitutes sulfur.

(c) The Raman shift of the weak bands detected in the 0–150 cm^{-1} region decreases as the metal cation mass increases.[10,26]

However, this model does not give the actual ion vibrations in the crystal. Future work will concentrate on lattice dynamics calculations in order to get a more realistic picture of the MPX_3 lattice vibrations.

In Figs. 3 and 4 the $FePS_3$ and $FePSe_3$ Raman spectra at room (a) and liquid helium (b) temperatures are shown. They are excited by the 488.0 nm and the 476.5 nm lines of an Ar^+ laser. The peak frequencies are given in Table

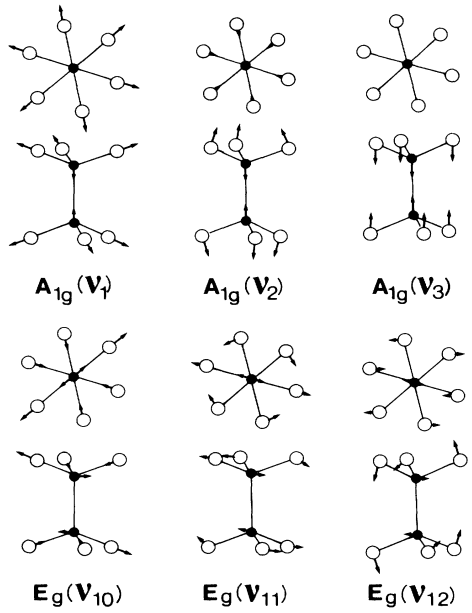

FIG. 2. The six Raman modes of the ethanelike X_2Y_6 molecule (D_{3d} group) (Ref. 25).

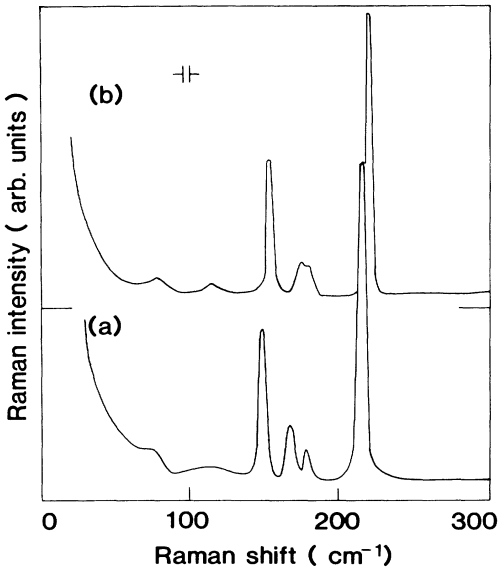

FIG. 4. Raman spectra of $FePSe_3$ recorded at room temperature (a) and at liquid helium temperature (b), excited by the 476.5-nm line of an Ar^+ laser.

I, and are compared with the calculated P_2S_6 normal mode frequencies reported in Ref. 10. Experiments with parallel or cross polarizations are carried out also, and the results are shown in Table I.

On the basis of the present experiments and of previous analysis,[9,10] the Raman peaks can be assigned as follows. A weak fine structure occurs around 580 cm^{-1} in $FePS_3$ at liquid helium temperature, whereas only a weak band is observed at 573 cm^{-1} in the room temperature experiments. The frequency of this structure fits quite well the $E_g(\nu_{10})$ mode frequency which has been calculated by different authors.[10,27] Slight lattice distortions could be responsible for the observed splitting.

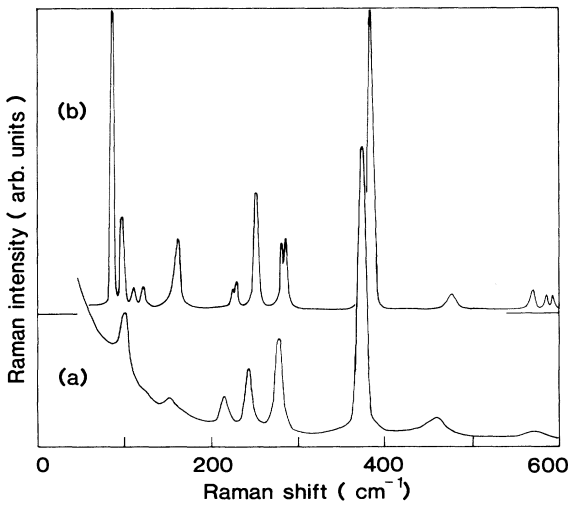

FIG. 3. Raman spectra of $FePS_3$ recorded at room temperature (a) and at liquid helium temperature (b), excited by the 448.0 nm line of an Ar^+ laser.

A weak peak, which has not been observed before in $FePS_3$, is detected at 480 cm^{-1}. In infrared absorption experiments a band has been found around this frequency[10] and assigned to the $A_{1g}(\nu_3)$ mode, which involves mainly the P—P bond stretching. Neither the $E_g(\nu_{10})$ nor the $A_{1g}(\nu_3)$ mode are found in the $FePSe_3$ Raman spectra.

The intense peaks at 380 cm^{-1} and at 221 cm^{-1} in the $FePS_3$ and $FePSe_3$ spectra, are strongly polarized. They are assigned to the $A_{1g}(\nu_1)$ mode of the P_2X_6 group, the symmetric stretching vibration of the P—X bonds. At room temperature the 275 cm^{-1} and 215 cm^{-1} peaks in the $FePSe_3$ spectrum and the corresponding peaks at 180 cm^{-1} and 149 cm^{-1} in the $FePSe_3$ spectrum are depolarized. At low temperatures in $FePS_3$ they are split in two components, which are active in two orthogonal scattering geometries. They are assigned to the $E_g(\nu_{11})$ and $E_g(\nu_{12})$ modes, respectively.

At liquid-helium temperature the bands at 249 cm^{-1} in $FePS_3$ and at 174 cm^{-1} in $FePSe_3$ are not observed in cross polarization measurements. Moreover in MPS_3 compounds, this band has been found very sensitive to alkali-ion intercalation and to the c-axis expansion.[28] They can be assigned to the $A_{1g}(\nu_2)$ mode (Fig. 2).

The frequency ratios between the P_2S_6 modes and the P_2Se_6 modes are found equal to 1.72, 1.56, 1.43, and 1.50 for the $A_{1g}(\nu_1)$, $E_g(\nu_{11})$, $A_{1g}(\nu_2)$, and $E_g(\nu_{12})$, respectively, in good agreement with the inverse square root of the chalcogen mass ratio (1.57).

One can remark that this systematics is better verified by the $E_g(\nu_{11})$ and $E_g(\nu_{12})$ modes which do not involve P—X bond stretchings.

At low temperature the band at 161 cm^{-1} is strongly enhanced in $FePS_3$ and appears depolarized. Only a very

TABLE I. Raman shifts at room and liquid helium temperature of $FePS_3$ and $FePSe_3$. The assignment in terms of normal modes of the P_2S_6 cluster is reported as well as the frequencies calculated by Sourisseau *et al.* (Ref. 10). (s=strong, m=medium, w=weak, p=polarized, dp=depolarized).

$FePS_3$		$FePSe_3$			$\nu_{(Calc.)}$	P_2X_6 normal
RT	LHT	RT	LHT	$\nu_{FePS_3}/\nu_{FePSe_3}$	(Ref. 10)	modes (Ref. 25)
	594w					
573w	582w				564	$E_g(\nu_{10})$
	564w					
466w	480w				434	$A_{1g}(\nu_3)$
376s	380s (p)	215s	221s	1.72	377	$A_{1g}(\nu_1)$
275m	283m (dp) 280m	180m	181m	1.56	262	$E_g(\nu_{11})$
243m	249m (p)	168m	174m	1.43	149	$A_{1g}(\nu_2)$
215w	231w 229w (dp)	149w	153w	1.50	171	$E_g(\nu_{12})$
150w	161m (dp)	110w	116w			
118w	120w					
	109w					
100w						
	95m (dp)					
	88s (dp)	78w	82w			

weak structure is found around 150 cm^{-1} in the room-temperature spectra of $FePS_3$,[9,10] of mixed $Fe_{1-x}Zn_xPS_3$,[29] and of other MPS_3 compounds.[26] It is the Raman counterpart of the strongly ir active $E_u(\nu_9)$-type mode of the P_2S_6 molecule observed in all the MPS_3 compound absorption spectra at about 155 cm^{-1}.[10]

Two strong peaks at 88 cm^{-1} and 95 cm^{-1} and two weaker structures at 120 cm^{-1} and 109 cm^{-1} appear in the $FePS_3$ spectrum at low temperature. The peaks at 88, 95, and 109 cm^{-1} decrease in intensity around the Néel temperature and only a broad band centered at 100 cm^{-1} is found at room temperature. No similar effect occurs in the selenide spectrum, where only two weak bands appear at 116 cm^{-1} and 82 cm^{-1} at liquid-helium temperature [Fig. 4(b)], and at 110 cm^{-1} and 78 cm^{-1} at room temperature [Fig. 4(a)].

The cation substitution effects are observed mainly below 150 cm^{-1}.[10,26] Some bands in the infrared and Raman spectra of the transition-metal phosphorus trichalcogenides shift to lower frequencies as the cation mass increases.[26] For this reason these structures have been assigned to vibrational modes which involve mainly the metal cation vibrations.[10,26] Our preliminary results on the mixed $Fe_{1-x}Zn_xPS_3$ compounds support this assignment. At room temperature a one mode behavior is found for the broad unresolved band around 100 cm^{1-} in $FePS_3$, which shifts up to 77 cm^{-1} and narrows as zinc substitutes iron.[29] However the large frequency shift (23 cm^{-1}) cannot be accounted for only by the mass differency. Stronger metal-sulfur bonds in the iron phosphorus trisulfide, due to partially covalent bonds, are responsible for this effect.

MAGNETIC ORDERING EFFECTS

$FePS_3$ and $FePSe_3$ Raman spectra are recorded at different temperatures to investigate the magnetic ordering effects. Dramatic modifications occur in the $FePS_3$ spectra around the Néel temperature, whereas the $FePSe_3$ spectrum is almost completely unaffected by the magnetic ordering.

In Fig. 5 iron phosphorus trisulfide Raman spectra are shown at different temperatures. The integrated intensities of the 380-, 249-, and 88-cm^{-1} peaks, corrected for the Bose population factor and normalized to the intensity extrapolated at T=0 K, are reported in Fig. 6. The 380-, 249-, and 88-cm^{-1} peak bandwidths, corrected for the slit width, are shown in Fig. 7. All the intensity-versus-temperature data are taken by increasing progressively the

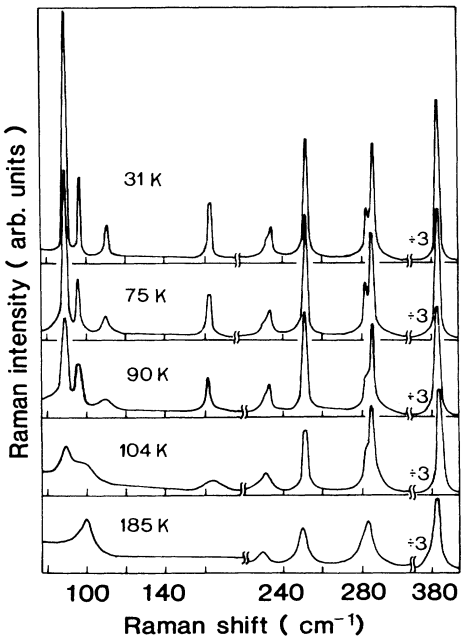

FIG. 5. Raman spectra of $FePS_3$ recorded at different temperatures using 488.0 nm laser excitation (T_N=118 K).

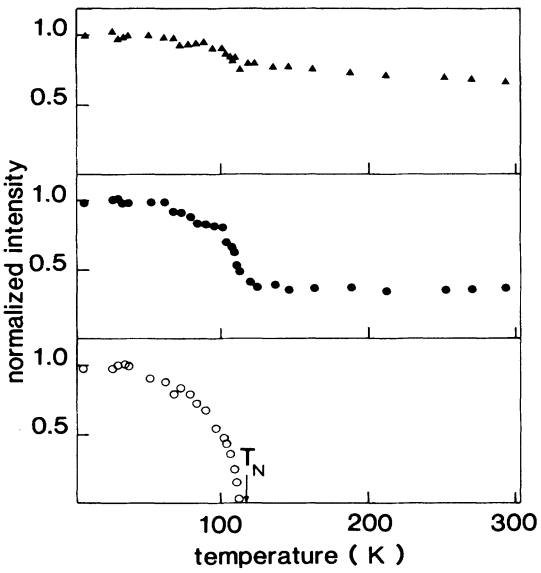

FIG. 6. Temperature dependence of the reduced integrated intensities $I(T)/I(0)$ of the peaks at 88 cm^{-1} (○), 249 cm^{-1} (●), and 380 cm^{-1} (▲) in the spectrum of $FePS_3$, excited by the 488.0 nm line. $I(0)$ is the value extrapolated at $T=0$ K.

sample temperature. We are not able, in the limit of the experimental error, to detect hysteresis phenomena at the transition temperature. Small hysteresis effects have been observed however in Mössbauer measurements.[5]

Peak narrowings and intensity enhancements occur at $T < T_N$ (118 K). The strong peak at 380 cm^{-1} slightly decreases in intensity (about 30%) around $T_{\text{Néel}}$ without anomalous broadening. On the other hand the intensity of the peak at 249 cm^{-1} decreases of about 60% and the

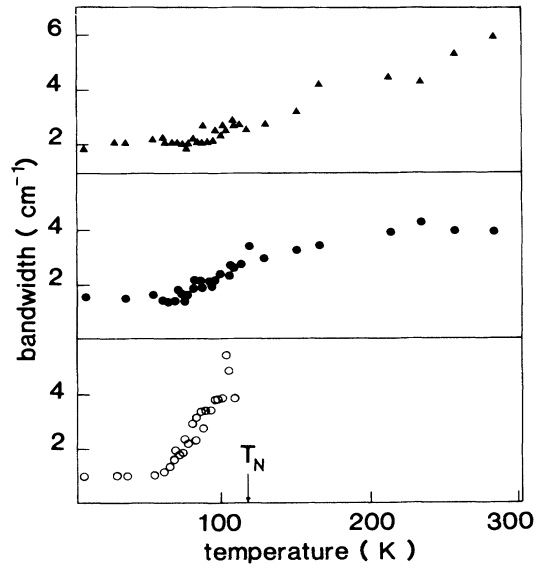

FIG. 7. Temperature dependence of the bandwidths of the peaks at 88 cm^{-1} (○), 249 cm^{-1} (●), and 380 cm^{-1} (▲) in the Raman spectra of $FePS_3$, excited by the 488.0 nm line.

bandwidth seems to exhibit a singularity going through the magnetic transition (Fig. 7). The E_g modes at 229–231 cm^{-1} and 280 cm^{-1} appear split into two components, and slightly enhanced at $T < T_N$ (Fig. 5).

The splitting of these bands is due to the band narrowing rather than to structural changes associated to the magnetic transition. In effect it occurs also in $ZnPS_3$.[26]

The most spectacular effects are found in the low frequency region of the spectrum. Three well resolved and strong peaks at 88, 95, and 109 cm^{-1} appear at $T < T_N$, instead of the broad unresolved band observed around 100 cm^{-1} in the paramagnetic phase. A strong band is found also at 161 cm^{-1}, corresponding to the room temperature band around 150 cm^{-1}. Preliminary measurements at liquid helium temperature on $Fe_{0.8}Zn_{0.2}PS_3$ show enhancements and appearance of new peaks around 100 cm^{-1}, but with intensity comparatively lower.

All these structures have vibrational origin. The bands at 88, 95, and 109 cm^{-1} and at lesser degree the band at 161 cm^{-1}, broaden around T_N (Fig. 7), but do not shift in frequency (Fig. 5), ruling out the hypothesis of one or two-magnon Raman scattering. Magnon bands generally broaden and exhibit frequency softening near the magnetic ordering temperature.[30]

It is also unlikely that these narrow bands (a bandwidth of about 1 cm^{-1} is evaluated at liquid-helium temperature) originate from electronic transitions.

The electronic excitations within the $^5T_{2g}$ ground state of the Fe^{2+} ion in an octahedral site have been recently observed in the Raman spectra of iron doped CdI_2.[31] For metal-cation concentrations larger than 2 at. % these bands broaden, and the fine structure due to the trigonal distortion of the iron-site symmetry becomes unresolved.[31]

A strong dependence of the vibrational cross section on the degree of magnetic ordering has been observed in magnetic crystals such as the ferromagnetic spinels $CdCr_2X_4$ (X=S,Se),[15–17] the iron dihalides $FeCl_2 \cdot 2H_2O$ (Ref. 18) and FeF_2,[32] the vanadium dihalides[12,13] and the 1D magnetic compound $CsCoBr_3$.[33,34]

In $CdCr_2S_4$ and $CdCr_2Se_4$ however, resonance effects on electronic levels undergoing splitting and shifts at T_C are partially responsible for the observed enhancements, as pointed out by Koshizuka and co-workers.[17] Although large shifts in the electronic levels at the transition temperature are observed more frequently in ferromagnetic compounds, measurements are carried out with different Ar^+ and Kr^+ laser lines from 647.1 to 457.9 nm to check this hypothesis.

The temperature dependence of the 88 and 95-cm^{-1} peak intensities is studied by means of the laser lines at 647.1, 514.5, and 476.5 nm, and it is found independent of the exciting wavelength. Moreover at liquid-helium temperature the intensity of the peaks at 88, 95, and 161 cm^{-1} is roughly independent of the exciting wavelength in the (1.92–2.71)-eV region, which corresponds to the d-d transitions, partially superimposed to the charge transfer transitions.[35] Only the peak at 380 cm^{-1} [$A_{1g}(\nu_1)$] exhibits a resonant behavior at the onset of the charge transfer transitions, but it is not surprising because of the different energy denominators in the spin-dependent and in the spin-independent terms of the Ra-

man tensor.[11] One can conclude that the temperature behavior of the $FePS_3$ spectrum is not due to shifts in the electronic levels involved as intermediate states in the Raman scattering process.

Useful suggestions to understand the strong spin dependent scattering can be obtained by the inspection of the $FePS_3$ infrared absorption spectrum.[10] It has been found that under certain conditions the magnetic superstructure can activate zone boundary phonons.[12–14] The modulation of the exchange interactions by these lattice modes provides an additional term to the phonon Raman tensor. Zone-boundary acoustic modes and infrared active optic modes can then be observed in the Raman spectra.

Now the $FePS_3$ magnetic cell is doubled along the c axis with respect to the crystallographic one, i.e., the A point is folded in Γ in the Brillouin zone below the ordering temperature. The observed intensity enhancement of the 161 cm^{-1} peak probably originates from this folding. In effect, the $E_u(\nu_9)$ mode which is infrared active with a frequency of 153 cm^{-1} at room temperature,[10] becomes Raman active when the unit cell is doubled along the c axis in the antiferromagnetic phase as shown in Fig. 8. Along the line of Δ the phonon dispersion curves in layered compounds are flat and this explains the very small shifts between the activated Raman line around 161 cm^{-1} and the corresponding infrared band. Also the $A_{1g}(\nu_2)$ mode at 249 cm^{-1} is strongly activated (Fig. 6). This mode presents a large component of the ions vibration along the c axis (Fig. 2) and it is also very sensitive to the interlayer magnetic coupling in the magnetic superstructure.

The scattering mechanism discussed in Ref. 12 can account for the appearance of the strong peaks at 88 and 95 cm^{-1} in the magnetic phase, although in the lack of phonon dispersion curves, a careful assignment of these peaks is difficult. The comparison with the lattice dynamics of similar compounds can be useful. Taking transition-metal dihalides as a reference (Fig. 9),[36] it can be seen that the substitution of one third of iron ions with phosphorus dimers reduces the Brillouin zone volume to one third. Particularly the K point is folded in Γ and the low-frequency A_2 and E acoustic modes become zone center modes. They are however only infrared active, and one of them could correspond to the weak infrared band observed in $FePS_3$ at 76 cm^{-1}.[10] At the same time the H and H' points are folded in A. Now the magnetic superstructure folds again A in Γ and the original A_2 and E modes can be activated in Raman. The frequency discrepancy is not surprising here because of the acoustic nature of these modes, which display some dispersion along the line of Δ.

Moreover they are expected to be depolarized and it is in agreement with the observation of the two bands at 88 and 95 cm^{-1} both in parallel and cross-polarization geometries. The splitting is probably due to the degeneracy lifting induced by lattice distortions.

As shown in Fig. 7 the peaks activated in the magnetic phase exhibit line broadening. This behavior probably originates from the coexistence in the same crystal of paramagnetic and antiferromagnetic phases around the ordering temperature, which has been put in evidence by Mössbauer measurements.[5]

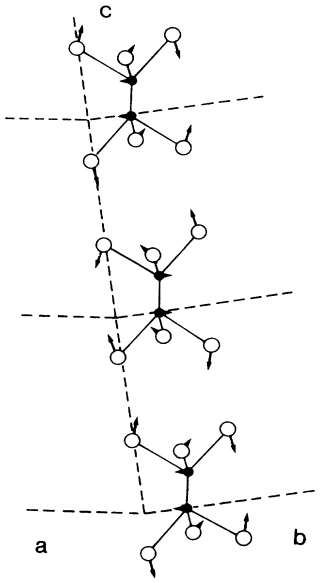

FIG. 8. Infrared active $E_u(\nu_9)$ mode of the X_2Y_6 molecule from Ref. 25. When the unit cell is doubled along the c axis the out-of-phase vibration of two X_2Y_6 groups in adjacent layers becomes Raman active.

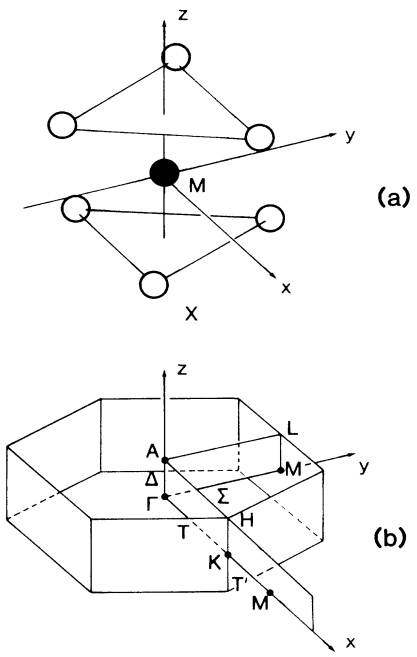

FIG. 9. (a) Octahedral cage of anions surrounding the metal ion in the $C6$ and $C19$ structures of the transition-metal dihalides. (b) The Brillouin zone of a lattice with the CdI_2 ($C6$) structure, in which the unit cell contains only one layer along the c axis (from Ref. 36).

The iron phosphorus triselenide Raman spectrum does not display strong spin-dependent behavior around the Néel temperature ($T_N = 106$ K). Only small frequency shifts and intensity changes occur as the temperature increases from 4.2 to 300 K. The reasons for this different behavior should be researched firstly in the larger interionic distances in the selenide, and consequently in weaker magnetic couplings[1] and also in the larger crystallographic cell, which contains three layers in the selenide. The magnetic cell is doubled along the c axis with respect to the crystallographic one in the selenide also, but in this case zone-boundary phonons do not provide the necessary modulation of the exchange interaction.

In effect, zone-boundary phonons activated by the Brillouin-zone folding can be observed only in $FePS_3$. Both nickel and cobalt phosphorus trichalcogenides have similar magnetic structure in the ab plane, but the near neighbor interplanar chains are coupled ferromagnetically, so that the magnetic cell is not doubled along the c axis. In the manganese compounds each magnetic ion is coupled antiferromagnetically with the three near neighbors and the crystallographic and the magnetic unit cells are identical.

A general theory which accounts for the temperature dependence of the integrated intensities of phonon Raman scattering in magnetic crystals has been formulated by Suzuki and Kamimura.[11] Starting from the polarization tensor of a magnetic compound in the form proposed by Moriya,[37] they have derived the following expression for the integrated phonon Raman scattering intensity $I(T)$:

$$I(T)=(n_0+1)\left[\left|R+M\frac{\langle \mathbf{S}_0\cdot\mathbf{S}_1\rangle}{S^2}\right|^2+|k|^2\langle S_z\rangle^2\right], \quad (1)$$

where R represents the ordinary spin-independent Raman tensor and n_0 is the Bose population factor. The last term is associated with the spins of single ions and with the electron-phonon interaction which is given by the variation of the spin-orbit interaction with the relative displacements of the ions. Its order of magnitude is determined essentially by spin-orbit coupling constant in the virtually excited state. Generally it is at least one or two orders of magnitude smaller than the other two terms, and it can be neglected.[11] The second term arises from the contribution to the polarizability tensor of the type $\sum_{i,j} R_{ij}(\mathbf{S}_i\cdot\mathbf{S}_j)$, where the nearest neighbor approximation is considered for the spin pairs. It has been shown that both the modulation of the d-electron transfer energy and of the nondiagonal exchange interaction by the lattice vibrations can contribute to this term.

By using the expression (1), the reduced spin-correlation function of $FePS_3$ is evaluated. The data reported in Fig. 10 are obtained from the intensity of the peak at 249 cm^{-1}. A R/M ratio of about 2.43 is found. The square of the reduced magnetic moment evaluated by neutron diffraction measurements[2] is reported also for comparison (Fig. 10). It represents the spin correlation when an infinite number of neighbors is considered, i.e., the lower bound for the spin correlation function. The two functions are constant up to $0.5-0.6T_N$, and abruptly decrease around T_N in agreement with the 2D Ising character of $FePS_3$. They are slightly different however in the range $0.6-0.9T_N$, where the spin correlation function decreases more smoothly. As expected the spin-correlation function is different from zero at $T > T_N$, due to local magnetic order. The peak at 380 cm^{-1} ($R/M=5.85$) as well as those at 88 and 161 cm^{-1} ($R/M=0$) (Ref. 9) display a similar behavior.

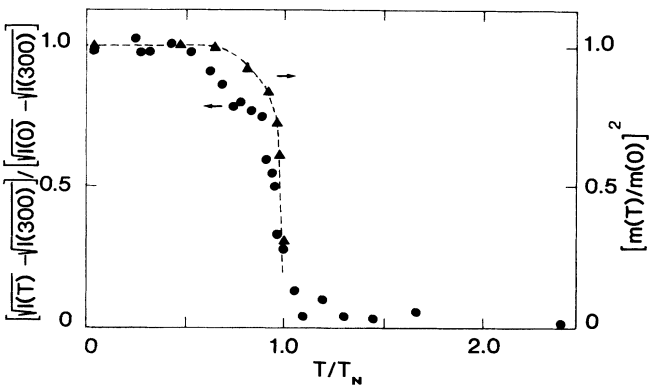

FIG. 10. Reduced nearest-neighbor spin-correlation function obtained from the temperature dependence of the intensity of the phonon at 249 cm^{-1} (●), in the spectrum of $FePS_3$ (see Fig. 6). The square of the reduced magnetization $m(T)/m(0)$ (▲) is reported for comparison (Ref. 2). The dashed line is shown as a visual aid.

CONCLUSIONS

The Raman spectra of iron phosphorus trichalcogenides single crystals are measured at different temperatures in the range 4.2–300 K. The Raman peaks are assigned to the normal modes of the $(P_2S_6)^{4-}$ anions and to phonons involving mainly the iron cation vibrations. Measurements with cross and parallel polarization in a quasiback-scattering geometry let us reconsider and correct some previous assignments.

Around the Néel temperature strong intensity enhancements are observed in the spectrum of the iron phosphorus trisulfide, while new peaks appear in the region 80–200 cm^{-1}. The temperature dependence of the integrated intensity, bandwidth and frequency is studied and correlated with the antiferromagnetic order. All the enhanced peaks have vibrational origin. Magnon scattering, resonant phonon Raman scattering on electronic levels that shift at T_N, and scattering associated to phase transitions, can be excluded on the basis of this work and of the present knowledge on the $FePS_3$ properties. It is suggested that the abrupt appearance of new lines in the low-frequency region of the spectrum is related to zone-boundary phonons activated by the magnetic superstructure. This hypothesis is supported by the available infrared data and by the investigation of Raman scattering polarization.

The general theory on phonon Raman scattering in magnetic crystals formulated by Suzuki and Kamimura[11] successfully accounts for the temperature behavior. The spin-correlation function of $FePS_3$ is evaluated from the 249-cm^{-1} peak temperature dependence. Its shape is consistent with the 2D Ising character of this layered magnetic compound.

Lattice-dynamics calculations are now in progress. They could further confirm the interpretation of the spin-dependent Raman scattering in $FePS_3$ in terms of zone-boundary phonons activated by magnetic ordering, and let us assign more carefully the low-frequency Raman bands.

ACKNOWLEDGMENTS

This work was supported in part by French "Direction de la Coopération Scientifique et Technique du Ministère des Relations Extérieures" and by the European Economic Community under Contract No. ST2P-0013-1-FR(CD). One of us (M.S.) wishes to thank the Université de Paris VI and Professor M. Balkanski for giving him the opportunity to work in the Laboratoire de Physique des Solides (Paris VI). Laboratoire de Physique des Solides is Unité Associé au Centre National de la Recherche Scientific (CNRS) No. 154. Laboratoire de Chimie des Solides is Unité Associé au CNRS No. 278.

*Present address: Cise-Tecnologie Innovative S.p.A., via Reggio Emilia 39, 20090 Segrate (Milano), Italy.

[1]G. Le Flem, R. Brec, G. Ouvrard, A. Louisy, and P. Segransan, J. Phys. Chem. Solids **43**, 455 (1982).

[2]K. Kurosawa, S. Saito, and Y. Yamaguchi, J. Phys. Soc. Jpn. **52**, 3919 (1983).

[3]A. Wiedenmann, J. Rossat-Mignod, A. Louisy, R. Brec, and J. Rouxel, Solid State Commun. **40**, 1067 (1981).

[4]K. Okuda, K. Kurosawa, and S. Saito, in *High Field Magnetism*, edited by M. Date (North-Holland, Amsterdam, 1983), p. 55.

[5]P. Jernberg, S. Bjarman, and R. Wappling, J. Magn. Magn. Mater. **46**, 178 (1984).

[6]A. H. Thompson and M. S. Whittingham, Mater. Res. Bull. **12**, 741 (1977).

[7]R. Brec, G. Ouvrard, A. Louisy, J. Rouxel, and A. Le Mehauté, Solid State Ionics **6**, 185 (1982).

[8]A. Le Mehauté, G. Ouvrard, R. Brec, and J. Rouxel, Mater. Res. Bull. **12**, 1191 (1977).

[9]M. Scagliotti, M. Jouanne, M. Balkanski, and G. Ouvrard, Solid State Commun. **54**, 291 (1985).

[10]C. Sourisseau, J. P. Forgerit, and Y. Mathey, J. Solid State Chem. **49**, 134 (1983).

[11]N. Suzuki and H. Kamimura, Solid State Commun. **11**, 1603 (1972); J. Phys. Soc. Jpn. **35**, 985 (1973).

[12]G. Güntherodt, W. Bauhofer, and G. Benedek, Phys. Rev. Lett. **43**, 1427 (1979).

[13]W. Bauhofer, G. Güntherodt, E. Anastassakis, A. Frey, and G. Benedek, Phys. Rev. B **22**, 5873 (1980).

[14]G. Güntherodt, G. Abstreiter, W. Bauhofer, G. Benedek, and E. Anastassakis, J. Magn. Magn. Mater. **15-18**, 777 (1980).

[15]E. F. Steigmeier and G. Harbeke, Phys. Kondens. Materie **12**, 1 (1970).

[16]N. Koshizuka, Y. Yokoyama, and T. Tsushima, Solid State Commun. **23**, 967 (1977); Physica B **89**, 214 (1977).

[17]N. Koshizuka, S. Ushioda, and T. Tsushima, Phys. Rev. B **21**, 1316 (1980).

[18]L. Graf and G. Schaack, in *The 3rd International Conference on Light Scattering in Solids (Campinas, 1975)*, edited by M. Balkanski, R. C. C. Leite, and S. P. S. Porto (Flammarion, Paris, 1976), p. 264.

[19]D. Ullrich, R. Courths, and C. von Grundherr, Physica B **89**, 205 (1977).

[20]P. Ferloni (private communication).

[21]R. W. G. Wychoff, *Crystal Structures* (Wiley, New York, 1984), Vol. II, p. 55.

[22]W. Klingen, Ph.D. thesis, Universitat Hohenheim, 1969.

[23]W. Klingen, G. Eulenberger, and H. Hahn, Z. Anorg. Allg. Chem. **401**, 97 (1973); W. Klingen, R. Ott, and H. Hahn, Z. Anorg. Allg. Chem. **396**, 271 (1973).

[24]R. Brec, G. Ouvrard, and J. Rouxel, Mater. Res. Bull. **20**, 1257 (1985); G. Ouvrard, R. Brec, and J. Rouxel, Mater. Res. Bull. **20**, 1181 (1985).

[25]G. Herzberg, *Infrared and Raman Spectra of Polyatomic Molecules*, 3rd. ed. (Van Nostrand, New York, 1947).

[26]Y. Mathey, R. Clement, C. Sourisseau, and G. Lucazeau, Inorg. Chem. **19**, 2773 (1980).

[27]R. Mercier, J. P. Malugani, B. Fahys, J. Douglade, and G. Robert, J. Solid State Chem. **43**, 151 (1982); H. Burger and H. Falius, Z. Anorg. Allg. Chem. **363**, 24 (1968).

[28]M. Barj and G. Lucazeau, Solid State Ionics **9-10**, 475 (1983).

[29]M. Scagliotti and M. Jouanne (unpublished).

[30]See, for example, D. J. Lockwood, in *Light Scattering in Solids III*, edited by M. Cardona and G. Güntherodt (Springer-Verlag, Berlin, 1982), p. 59.

[31]I. W. Johnstone and L. Dubicki, J. Phys. C **13**, 121 (1980).

[32]D. J. Lockwood, R. S. Katiyar, and V. C. Y. So, Phys. Rev. B **28**, 1983 (1983).

[33]D. J. Lockwood, in *Magnetic Excitations and Fluctuations*, edited by S. W. Lovesey *et al.* (Springer-Verlag, Berlin, 1984), p. 33.

[34]I. W. Johnstone, D. J. Lockwood, and L. Dubicki, J. Magn. Magn. Mater. **15-18**, 799 (1980).

[35]M. Piacentini, F. S. Khumalo, G. Leveque, C. G. Olson, and D. W. Lynch, Chem. Phys. **72**, 61 (1982); V. Grasso, S. Santangelo, and M. Piacentini, Solid State Ionics **20**, 9 (1986).

[36]G. Benedek and A. Frey, Phys. Rev. B **21**, 266 (1980).

[37]T. Moriya, J. Phys. Soc. Jpn. **23**, 490 (1967).